Analytical Study of Performances of Monolayer and Bilayer Graphene FETs Based on Physical Mechanisms

J.D. Aguirre-Morales, C. Mukherjee, S. Fregonese, C. Maneux and T. Zimmer
IMS Laboratory, UMR CNRS 5218, Cours de la Libération – 33405 Talence Cedex, Bordeaux, France
jorge.aguirre@ims-bordeaux.fr

Abstract
Following the recents works of K.S. Novoselov and A.K. Geim [1] in 2004, the semiconductor industry has been attracted to carbon-based technologies in order to maintain the trend on low-cost and still reducible transistor structures. From circuit point of view, monolayer and bilayer Graphene FETs (GFETs) are being studied for high performance applications. Although monolayer graphene presents an energy band structure where there is no bandgap, its high thermal and electrical conductivity makes it suitable for high-frequency applications. On the other hand, bilayer graphene presents a tunable bandgap by the application of an electric field perpendicular to the layer which allows the design of more flexible GFET structures. In this paper, we report the evidence of a tunable bandgap on bilayer graphene based on physical equations and the expected performances of these devices are compared with monolayer graphene FETs. The presented results are based on GFET structures with an HfO_2 top gate dielectric ($\varepsilon_r = 16$) and a SiO_2 back gate dielectric ($\varepsilon_r = 3.9$) as in [4]. The gate length is fixed to 1 µm and the width to 2.1 µm. Residual carrier density n_{puddle} is considered to be 1.5e12 cm^{-2} and the net doping concentration to -5e12 cm^{-2}. Access resistances R_S and R_D are set to be equal to 100 Ω. Electron and hole mobilities are set to 1500 cm^2/V s.
For the simulations shown below, the effect of a tunable bandgap on a AB-stacking bilayer graphene (Figure 1) due to the applied electric field has been taken into account. Figure 2 shows the low energy bands for bilayer graphene for two different values of the applied potential energy. When the applied potential energy is zero (U = 0 eV) there is no bandgap ($E_{gap} = 0$), on the other hand when the applied potential energy is non-zero (i.e. U = 1 eV), the presence of a non-zero energy band gap can be observed. Figure 3 shows the Energy band gap E_{gap} under the average electrical displacement field generated by the applied bias voltages [2]. A variation on E_{gap} within [0 to 250 meV] can be noted. For the purpose of a comparative study, the monolayer and bilayer GFETs are compared via numerical simulations. Based on [3] and [4], a model for monolayer GFET has been developed where access resistances, the effect of puddles on carrier density and doping concentration are taken into account. In the case of bilayer GFETs a model based on physical equations [5] has been developed. Figure 4 shows a comparison of the I_{DS}-V_{GS} plot for bilayer and monolayer GFETs under the same bias conditions V_{DS} = [-1.5, -1.0, -0.5] V and a back-gate voltage V_{BG} = -40 V. Higher currents on bilayer GFETs can be observed from Figure 4 and a higher transconductance g_m reflecting a better current modulation in the channel by the gate voltage. Figure 5 shows the typical I_D-V_{DS} characteristic for both bilayer and monolayer GFETs under the same bias conditions Vgs = [0 to 3.0] V and V_{BG} = -40 V. Higher currents and higher output conductance g_{ds} are observed in the case of bilayer GFETs. The effect of a backgate voltage V_{BG} is shown in Figure 6 from which it can be observed that the current modulation stays constant for all V_{BG} as the ambipolar point (V_{Dirac}) moves along de x-axis. Extraction of small-signal parameters from both the GFETs allows us to calculate the cut-off frequency f_T as a function of gate length (Figure 7). Higher cut-off frequencies, f_T, can be observed for bilayer graphene for all gate lengths. Scaling down gate lengths for both bilayer and monolayer GFETs show an increase in f_T. Thus, from our study, we can infer some important conclusions about the possible future of GFETs as bilayer graphene offers higher cut-off frequencies and a tunable band gap over monolayer devices. Even if voltage gain ($A_V = g_m/g_{ds}$) is higher in bilayer graphene FETs, it is still to be improved for future high-performance applications.

Acknowledgements
This work (part of the GRADE project) was supported by the European Commission through the Seventh Framework Program for Research and Technological Development and by the French National Research Agency (ANR) through the P2N "GRACY" project.

References

[1] K. S. Novoselov, A.K. Geim, S.V. Morozov, D. Jiang, Y. Zhang, S.V. Dubonos, I.V. Grigorieva, Firsov and A.A. Firsov, *Science*, 5696 (2004) pp. 666-669.
[2] Y. Zhang, T. Tang, C. Girit, Z. Hao, M. Martin, A. Zetti, M. Crommie, Y. Shen and F. Wang, *Nature,* 459(2009), pp. 820-823.
[3] S. Fregonese, M. Magallo, C. Maneux, H. Happy and T. Zimmer, *IEEE Transactions on Nanotechnology*, 4 (2013), pp. 539-546.
[4] S.A. Thiele, J.A. Schaefer and F. Schwierz, *Journal of Applied Physics*, 9 (2010), p. 094505.
[5] M. Cheli, G. Fiori, G. Iannaccone, *IEEE Transactions on Electron Devices*, 12 (2009), pp. 2979-2986.

Figures

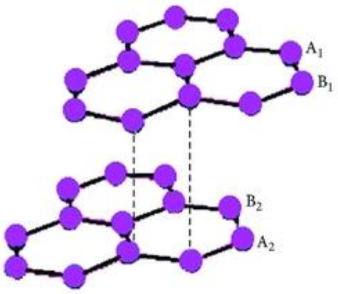

Figure 1: AB – stacking bilayer graphene

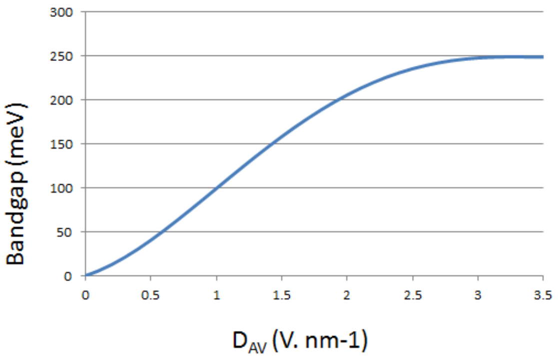

Figure 3: Bandgap variation under average electrical displacement fields

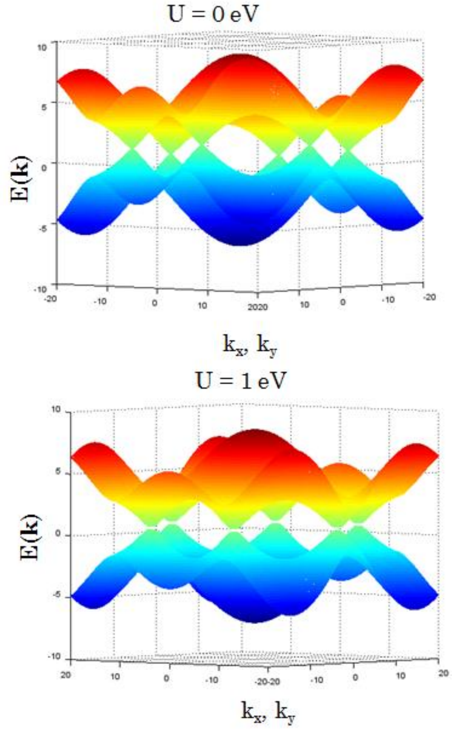

Figure 2: Low energy bands for bilayer graphene for two values of the applied potential energy

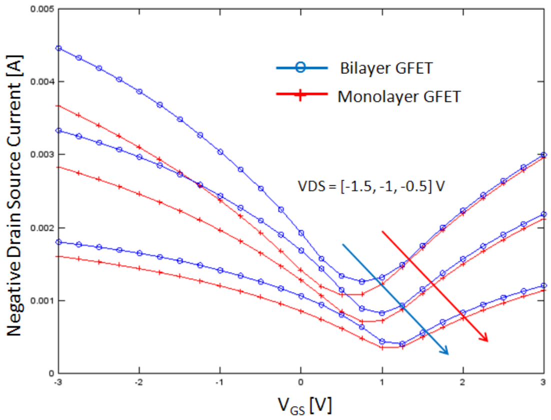

Figure 4: $I_{DS}(V_{GS})$ for monolayer (red) and bilayer (blue) GFETs for V_{DS} = [-1.5, -1.0, -0.5] V, V_{BG} = -40 V and $R_S = R_D$ = 100 Ω.

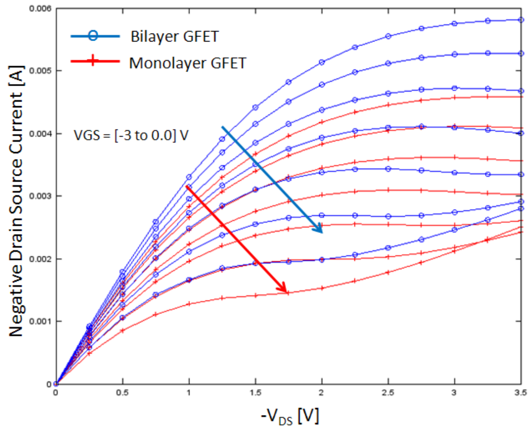

Figure 5: $I_{DS}(V_{DS})$ for monolayer (red) and bilayer (blue) GFETs for V_{GS} = [-3 to 0],V_{BG} = -40 V and $R_S = R_D$ = 100 Ω.

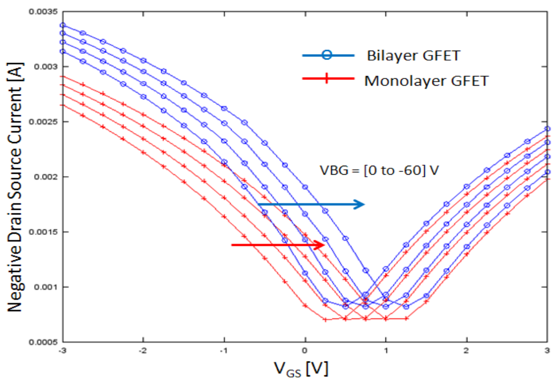

Figure 6: $I_{DS}(V_{GS})$ for monolayer (red) and bilayer (blue) GFETs for V_{DS} = -1.0 V, V_{BG} = [0 to -60] V and $R_S = R_D$ = 100 Ω.

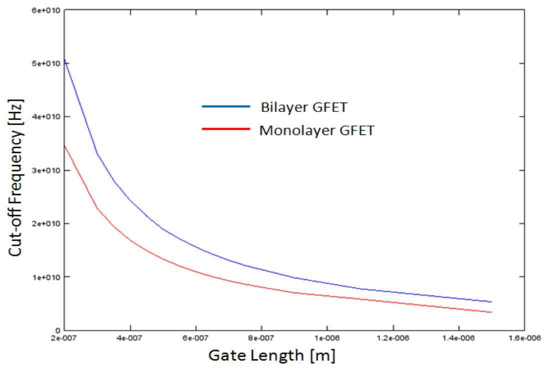

Figure 7: f_T as a function of gate length (L) for monolayer (red) and bilayer (blue) GFETs for V_{DS} = 1.0 V, V_{BG} = -40 V, V_{GS} = 0.5 V and R_S = R_D = 100 Ω.